Appl. Magn. Reson. 17, 197–209 (1999)

Applied Magnetic Resonance

Efficient Spin Diffusion of Transverse ^{13}C Magnetization

W.-G. Hu[1], H. Zimmermann[2], and K. Schmidt-Rohr[1]

[1] Department of Polymer Science and Engineering, University of Massachusetts, Amherst, Massachusetts, USA
[2] Max-Planck-Institut für Medizinische Forschung, Heidelberg, Germany

Received May 5, 1999; revised May 26, 1999

Abstract. Relatively efficient spin diffusion among unprotonated carbons with large chemical-shift anisotropies can be achieved by a ^{13}C nuclear magnetic resonance multiple-pulse sequence with a low-duty cycle of ~5% on the ^{13}C channel, which minimizes sample heating and reduces cumulative effects of pulse imperfections. The spin diffusion occurs among transverse-magnetization isochromats, while the total transverse magnetization is a conserved quantity under the average Hamiltonian. The "flip-flop" term of the dipolar-coupling average Hamiltonian is the same as in the full dipolar coupling, i.e., its scaling factor is unity. For a sample of 40% ^{13}COO-labeled poly(vinyl acetate), with ^{13}C in ester groups accounting for 7% of all heavy atoms, magnetization equilibrates within 20 ms over a volume of $(0.9\ nm)^3$, corresponding to a molecular mass of 500 Da, while the T_2 relaxation time of the total transverse magnetization is ~40 ms. The spin diffusion coefficient is estimated as $D = 3 \pm 1.5\ nm^2/s$.

1 Introduction

^{13}C magnetization exchange or spin diffusion in nonspinning samples is useful for characterizing the local structure in amorphous polymers [1–4] and for measuring the size of dynamic heterogeneities near the glass transition (K. Schmidt-Rohr et al., unpubl.), [5]. However, when the weak long-range ^{13}C-^{13}C dipolar couplings are smaller than the resonance mismatch due to chemical-shift differences of the coupled spins, dipolar exchange of longitudinal magnetization is very inefficient [3]. In other words, the dipolar Hamiltonian truncated by the chemical-shift difference does not produce exchange of longitudinal ^{13}C magnetization. Special radio-frequency (rf) pulse sequences are needed for reintroducing efficient ^{13}C spin exchange. Radio-frequency-driven spin diffusion [3, 4] achieves this by averaging out the chemical shift, using windowless spin-locking pulse sequences on ^{13}C. It requires delicate tuning of pulse phases and, with a 100% duty cycle on the ^{13}C channel for tens of milliseconds and simultaneous high-power ^1H decoupling, involves the risk of sample heating. In addition, the dipolar transfer rate is scaled down by 50% compared to the full dipolar Hamiltonian.

The finite lifetime of the dynamic heterogeneities near the glass transition [6] requires the fastest spin diffusion possible in experiments probing their size; in addition, the high sensitivity of the correlation times to temperature (a temperature raise by 4 K decreases the correlation times by a factor of three) requires strict avoidance of radio-frequency heating of the sample. In this paper, we demonstrate a pulse sequence [7, 8] which, based on average Hamiltonian theory [9–11], provides full, essentially unscaled dipolar spin diffusion between isochromats of transverse magnetization, while leaving the total transverse magnetization invariant (except for T_2 relaxation). The duty cycle on the ^{13}C channel is <5% at $\gamma B_1/2\pi = 60$ kHz, and only moderate 64 kHz continuous-wave proton decoupling is applied. Compared to radio-frequency-driven spin diffusion, the total rf energy in our new sequence is reduced by more than an order of magnitude. The experiments are demonstrated on amorphous poly(vinyl acetate), PVAc, in which 40% of the COO groups are ^{13}C-labeled, so that 7% of all heavy nuclei are ^{13}C.

2 Experimental

The nuclear magnetic resonance (NMR) experiments were performed on a Bruker MSL-300 spectrometer at a ^{13}C frequency of 75 MHz, in a static Bruker double-resonance probehead with an 8 mm diameter radio-frequency coil. The ^{13}C 90°-pulse length was 4.15 μs, the ^{1}H decoupling power $\gamma B_1/2\pi \approx 64$ kHz. No special tune-up of pulse phases or individual amplitudes was performed; only the 90°- and 180°-pulse lengths were adjusted carefully. Under these conditions, attempts at radio-frequency-driven spin diffusion were unsuccessful.

The measurements were performed at 276 K to avoid reorientations of the ^{13}COO groups in poly(vinyl acetate), $[\text{-}CH_2\text{-}CH\{\text{-}O\text{-}CO\text{-}CH_3\}\text{-}]_n$, on the 100 ms time scale. For the 2-D spectra, $96t_1$ increments of 20 μs were measured, with 128 scans per t_1 slice and a recycle delay of 6 s. The cross-polarization time was 2 ms. The evolution during t_1 was measured off-resonance, while the pulses after the z-period following t_1 were applied "on-resonance" (near the center of gravity of the ^{13}COO powder pattern). Gated decoupling of 26 μs was used before detection to suppress the natural-abundance ^{13}C signals of the CH_2, CH, and CH_3 sites.

2 Theory

2.1 Advantages of Transverse Magnetization Transfer

As is well known, the chemical-shift difference of two ^{13}C spins truncates a weak homonuclear dipolar coupling between the spins to a Hamiltonian that, under proton decoupling, does not produce transfer of z-magnetization. However, in combination with occasional 90° pulses, it is efficient at producing magnetization transfer among isochromats of transverse magnetization.

Consider as an example the time evolution of transverse magnetization of one spin in a system consisting of just two ^{13}C spins S and L (with chemical shifts

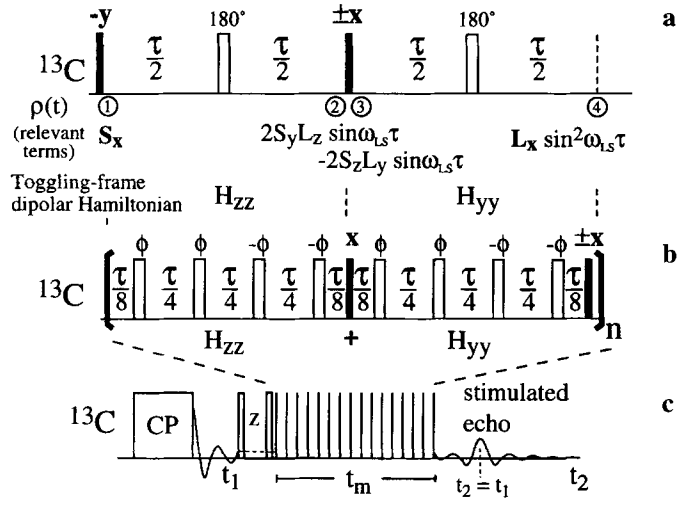

Fig. 1. **a** Pulse sequence for transfer of transverse magnetization in a ^{13}C spin pair. **b** Multiple-pulse sequence for transfer of transverse magnetization, leaving the total transverse magnetization invariant, apart from T_2 decay. The phase ϕ of the 180° pulses is fixed but arbitrary. **c** Pulse sequence for stimulated-echo and 2-D exchange experiments with the transverse spin diffusion sequence of **b** applied during the mixing time.

ω_S and ω_L) under the pulse sequence of Fig. 1a and the truncated dipolar Hamiltonian (i.e., in the weak-coupling limit) with the dipolar frequency

$$\omega_{SL} = \frac{-\mu_0}{4\pi}\frac{\hbar\gamma^2}{r_{SL}^3}\frac{1}{2}(3\cos^2\theta_{SL} - 1) \tag{1}$$

with the internuclear distance r_{SL}, the angle θ_{SL} between the S-L internuclear vector and the B_0 field, and the gyromagnetic ratio γ. The 180° pulses, given a sufficiently long $\tau/2 \gg 2\pi/|\omega_S - \omega_L|$ so that the truncation is not disturbed, simply refocus the chemical shift at the time of the 90°x pulse and before detection. Thus, we can disregard the chemical shift and consider purely dipolar evolution. We treat the case where only S_x magnetization is present initially:

$$\begin{aligned} S_x &\xrightarrow{\mathcal{H}_{zz}^{\text{trunc}}} S_x\cos\omega_{SL}\tau + 2S_yL_z\sin\omega_{SL}\tau \xrightarrow{90°x} S_x\cos\omega_{SL}\tau - 2S_zL_y\sin\omega_{SL}\tau \\ &\xrightarrow{\mathcal{H}_{zz}^{\text{trunc}}} \cos\omega_{SL}\tau(S_x\cos\omega_{SL}\tau + 2S_yL_z\sin\omega_{SL}\tau) \\ &\quad -\sin\omega_{SL}\tau(2S_zL_y\cos\omega_{SL}\tau - L_x\sin\omega_{SL}\tau) \\ &= S_x\cos^2\omega_{SL}\tau + L_x\sin^2\omega_{SL}\tau + (S_yL_z - S_zL_y)\sin\omega_{SL}2\tau\ . \end{aligned} \tag{2}$$

The term $L_x\sin^2\omega_{SL}\tau$ represents the transfer of transverse magnetization from spin S to spin L.

This pulse sequence provides efficient magnetization transfer between the two coupled spins. However, in the presence of more spins, unobservable multispin coherences develop quite fast and the observable magnetization disappears correspondingly. Therefore, the pulse sequence must be modified to ensure that the total transverse magnetization is conserved (apart from T_2 relaxation).

2.2 *Conserving the Total Transverse Magnetization*

In normal spin diffusion, the total z-magnetization

$$M = \sum_{n=1}^{N} S_z^n \quad , \tag{3}$$

which is proportional to the Zeeman Hamiltonian, is an invariant (apart from T_1 relaxation) since it commutes with the dipolar Hamiltonian $\mathscr{H}_{zz}^{\text{full}}$

$$[\mathscr{H}_{zz}^{\text{full}}, M] = \left[\sum_{j<k} \hbar\omega_{jk} (3S_z^j S_z^k - \mathbf{S}^j \cdot \mathbf{S}^k), \sum_{n=1}^{N} S_z^n \right] = 0 \quad . \tag{4}$$

Generally, if the Hamiltonian $\mathscr{H}$ and an observable M commute, the expectation value of M is invariant, according to

$$\begin{aligned} \langle M \rangle(t) &= \mathrm{Tr}\left(M\rho(t)\right) = \mathrm{Tr}\left(M \exp\left(-\frac{\mathrm{i}}{\hbar}\mathscr{H}t \right) \rho(0) \exp\left(\frac{\mathrm{i}}{\hbar}\mathscr{H}t \right) \right) \\ &= \mathrm{Tr}\left(\exp\left(\frac{\mathrm{i}}{\hbar}\mathscr{H}t \right) M \exp\left(-\frac{\mathrm{i}}{\hbar}\mathscr{H}t \right) \rho(0) \right) = \mathrm{Tr}\left(M\rho(0)\right) = \langle M \rangle(0) \quad , \end{aligned} \tag{5}$$

where we used Tr(AB) = Tr(BA) in the third and the commutation of $\mathscr{H}$ and M in the fourth step. Note that the individual $\langle S_z^n \rangle$ are time-dependent during spin diffusion; only their sum is invariant.

To achieve a similar invariance for the total transverse magnetization, we need a pulse sequence that generates an effective (average) Hamiltonian which commutes with the total x-magnetization, while transferring transverse magnetization between different isochromats. The total x-magnetization is invariant under

$$\mathscr{H}_{\text{trans}} = \frac{\tau}{2\tau} \sum_{j<k} \hbar 2\omega_{jk} (S_z^j S_z^k + \mathbf{S}_y^j \mathbf{S}_y^k) = \sum_{j<k} \hbar\omega_{jk} (-S_x^j S_x^k + \mathbf{S}^j \mathbf{S}^k) \quad , \tag{6}$$

because

$$\left[\sum_{j<k} \hbar\omega_{jk} (-S_x^j S_x^k + \mathbf{S}^j \mathbf{S}^k), \sum_{n=1}^{N} S_x^n \right] = 0 \quad , \tag{7}$$

and similarly the total x-magnetization commutes with, and is therefore invariant under

$$-\frac{1}{2}\mathcal{H}_{xx}^{\text{full}} = -\frac{\tau}{2\tau}\sum_{j<k}\hbar\omega_{jk}(3S_x^jS_x^k - \mathbf{S}^j\mathbf{S}^k) \quad . \tag{8}$$

As will be shown in the following, these Hamiltonians are obtained as average Hamiltonians in the weak- and very-strong-coupling limits, respectively, under the pulse sequence of Fig. 1b.

2.3 Transverse Spin Diffusion

The Hamiltonians of Eqs. (6) and (8) can be generated as average Hamiltonians by repeating the transfer pulse sequence of Fig. 1a multiple times with $\tau \ll 2\pi/\omega_{jk}$ (where $2\pi/\omega_{jk} > 1000$ μs for C-C distances >3.6 Å) so that the conditions of average Hamiltonian theory are fulfilled [9–11]. The resulting pulse sequence is shown in Fig. 1b. It was first introduced in solution NMR for advanced COSY experiments [8] and more recently applied to demonstrate spin waves in J-coupling-mediated spin exchange [7, 8]. The 180° pulses refocus the chemical shift periodically, if τ is chosen in the right range (see below). During the first τ, the Hamiltonian is the regular truncated dipolar Hamiltonian $\mathcal{H}_{zz}^{\text{trunc}} = \sum_{j<k}\hbar\omega_{jk}2S_z^jS_z^k$ in the weak-coupling limit, and $\mathcal{H}_{zz}^{\text{full}}$ in the very-strong-coupling limit. As always [9–11], the 90°-pulse propagators P_x and P_{-x}, which produce 90° rotations, can be applied to the density operator or to the propagators:

$$\begin{aligned}\rho(2n\tau) &= \left(\exp\left(-\frac{\mathrm{i}}{\hbar}\mathcal{H}_{zz}\tau\right)P_x\exp\left(-\frac{\mathrm{i}}{\hbar}\mathcal{H}_{zz}\tau\right)P_{-x}\right)^n S_x^j \\ &\quad\times\left(P_{-x}\exp\left(\frac{\mathrm{i}}{\hbar}\mathcal{H}_{zz}\tau\right)P_x\exp\left(\frac{\mathrm{i}}{\hbar}\mathcal{H}_{zz}\tau\right)\right)^n \\ &= \left(\exp\left(-\frac{\mathrm{i}}{\hbar}\mathcal{H}_{zz}\tau\right)\exp\left(-\frac{\mathrm{i}}{\hbar}\mathcal{H}_{yy}\tau\right)\right)^n S_x^j\left(\exp\left(\frac{\mathrm{i}}{\hbar}\mathcal{H}_{yy}\tau\right)\exp\left(\frac{\mathrm{i}}{\hbar}\mathcal{H}_{zz}\tau\right)\right)^n \quad . \end{aligned} \tag{9}$$

If the time τ is much shorter than the inverse dipolar coupling of $(50\ \text{Hz})^{-1} = 20$ ms, the usual average Hamiltonian approximation [9–11] can be applied:

$$\left(\exp(-\mathrm{i}\mathcal{H}_{zz}\tau/\hbar)\exp(-\mathrm{i}\mathcal{H}_{yy}\tau/\hbar)\right)^n \approx \left(\exp(-\mathrm{i}(\mathcal{H}_{zz}+\mathcal{H}_{yy})\tau/\hbar)\right)^n \quad . \tag{10}$$

Thus, with

$$\overline{\mathcal{H}} = \frac{1}{2}(\mathcal{H}_{zz}+\mathcal{H}_{yy}) \tag{11}$$

we have $\rho \approx \exp(-i\overline{\mathscr{H}}t/\hbar)S_x^j \exp(i\overline{\mathscr{H}}t/\hbar)$.

In the calculation above, it was assumed for convenience that the phases of the 90° pulses alternate. However, the dipolar coupling is invariant under a change of the pulse phase by 180° (e.g., from $-x$ to x). Therefore, the average Hamiltonian, Eq. (11), is unchanged if all the 90° pulses are x pulses. In practice, it is found that this produces much better results than with the original alternating x, $-x$ pulses. Possibly, this is because after a set of four x pulses, the average chemical-shift Hamiltonian during the pulses is zero.

2.4 *Weak-Coupling Limit*

In the weak-coupling limit, $\overline{\mathscr{H}} = (1/2)(\mathscr{H}_{zz} + \mathscr{H}_{yy})$ of Eq. (11) is the Hamiltonian $\mathscr{H}_{\text{trans}}$ of Eq. (6). This corresponds exactly to the "flip-flop" term in the dipolar Hamiltonian which is responsible for spin diffusion. As shown above, it transfers magnetization between isochromats but leaves the total transverse magnetization invariant. To ensure that the weak-coupling limit is valid, the pulse spacings must be considered carefully. In addition to $\tau \ll 2\pi/\omega_{jk} \sim 1$–$10$ ms (depending on the internuclear distance), we require $\tau/4 > 2\pi/|\omega_j - \omega_k| \sim 0.2$ ms in order to remain in the weak-coupling limit. The 180° pulses refocus the chemical shift periodically (but on a time scale longer than the inverse of the chemical-shift anisotropy $\Delta\omega_\sigma$) in the weak-coupling limit, which applies for most segments since the dipolar couplings are typically <50 Hz, much smaller than the chemical-shift differences, which are of the order of kHz given the chemical-shift anisotropy $\Delta\omega_\sigma = 11$ kHz. It would be sufficient to use one or two 180° pulses in the τ period rather than four. This would ensure the weak-coupling limit even better. The set of four 180° pulses was chosen here for compensation of pulse imperfections. Their phases x, x, $-x$, $-x$ were unchanged in different scans while the direction of the magnetization was cycled through the four quadrature directions. The data shown below were obtained with $\tau = 0.8$ ms.

To determine the scaling factor of the average Hamiltonian

$$\mathscr{H}_{\text{trans}} = -\sum_{j<k} \hbar\omega_{jk}(S_x^j S_x^k - \mathbf{S}^j\mathbf{S}^k) \tag{12}$$

acting on x-magnetization, we need to compare it with the full spin-diffusion Hamiltonian

$$\mathscr{H}_{zz}^{\text{full}} = \sum_{j<k} \hbar\omega_{jk}(3S_z^j S_z^k - \mathbf{S}^j\mathbf{S}^k) \tag{13}$$

acting on z-magnetization. Due to the different prefactors of $S_x^j S_x^k$ and $S_z^j S_z^k$, the comparison is not completely straightforward. For a system of more than two spins, $S_x^j S_x^k$ or $S_z^j S_z^k$ do not commute with other terms in the Hamiltonian and therefore do affect the time evolution. However, we note that the crucial terms

for transfer are the scalar products $\mathbf{S}^j\mathbf{S}^k$, while $S_x^jS_x^k$ or $S_z^jS_z^k$ commute with the initial density operator. Thus, we can disregard $S_x^jS_x^k$ or $S_z^jS_z^k$ in the initial regime and find that the most relevant scaling factor, for the dot-product or "flip-flop" terms, is unity. This scaling factor is confirmed by the two-spin density-operator treatment of Eq. (1), where the transfer occurs with $\sin^2(\omega_{CC}\tau)$, i.e., with the unscaled dipolar coupling. Whether a slightly larger prefactor of $S_x^jS_x^k$ or $S_z^jS_z^k$ speeds up or slows down spin diffusion is not clear a priori. It may be interesting to note that $S_x^jS_x^k$ or $S_z^jS_z^k$ with a very large prefactor would truncate the scalar product to a Hamiltonian that does not produce spin diffusion. Thus, the smaller prefactor of $S_x^jS_x^k$ in $\mathcal{H}_{trans}$ may help to keep spin diffusion efficient. In fact, a Hamiltonian very similar to $\mathcal{H}_{trans}$ has been shown to produce fast-traveling spin waves on a one-dimensional lattice [7, 12].

Note that a pure dot-product average Hamiltonian, though with a scaling factor of 2/3, could be generated with a pulse sequence similar to that of Fig. 1b, using the WHH-4 pulse sequence [9–11] for the 90° pulses, interspersed with 180° pulses to refocus the chemical-shift anisotropy in the windows.

In summary, even though the magnetization is transverse and not spin-locked, its effective time evolution is similar to that of z-magnetization under ideal spin diffusion (and about twice as fast as that of spin-locked magnetization). Therefore, we can treat this behavior like unscaled ^{13}C spin diffusion and will also refer to it as such.

2.5 Very-Strong-Coupling Limit

In the very-strong-coupling limit, i.e., for $\omega_{SL} \gg |\omega_S - \omega_L|$, the average Hamiltonian generated by the pulse sequence in Fig. 1b is $\overline{\mathcal{H}} = (-1/2)\mathcal{H}_{xx}^{full}$ as given in Eq. (8). This is derived easily from the magic zero of the dipolar coupling, $\mathcal{H}_{xx}^{full} + \mathcal{H}_{yy}^{full} + \mathcal{H}_{zz}^{full} = 0$. $\overline{\mathcal{H}} = (-1/2)\mathcal{H}_{xx}^{full}$ is the same Hamiltonian as under spin-lock conditions, and similarly conserves the total magnetization.

For a two-spin system, the dipolar $\mathcal{H}_{xx}^{full}$, $\mathcal{H}_{yy}^{full}$, and $\mathcal{H}_{zz}^{full}$ commute, and the average-Hamiltonian result, $\overline{\mathcal{H}} = (-1/2)\mathcal{H}_{xx}^{full}$, is exact. Thus, the two-spin time evolution under the sequences of Fig. 1a or b is

$$S_x \rightarrow S_x\cos^2\omega_{SL}\tau/2 + L_x\sin^2\omega_{SL}\tau/2 + (S_yL_z - S_zL_y)\sin^2\omega_{SL}\tau \ . \qquad (14)$$

As in the weak-coupling case, transfer of transverse magnetization, from S_x to L_x, is achieved.

3 Results and Discussion

Figure 2 shows the total transverse magnetization after application of the multiple-pulse sequence of Fig. 1b for a time τ_m, with a <5% duty cycle on the ^{13}C channel. It takes 27 ms for the magnetization to decay to half its initial value. This corresponds to a T_2 of ~40 ms, or a homogeneous linewidth of 8 Hz. Note

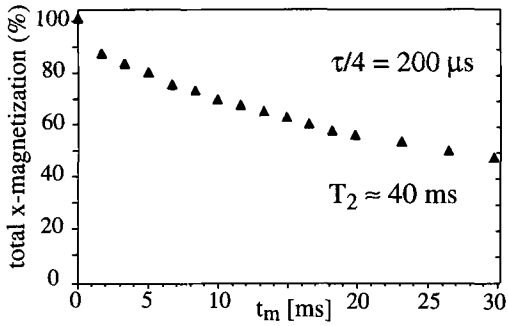

Fig. 2. T_2-decay of total transverse magnetization in ^{13}COO-PVAc under the multiple-pulse sequence of Fig. 1b as a function of the time t_m in the pulse sequence of Fig. 1c. The increment of t_m is a cycle time of $2t + 9t_{180} = 1.67$ ms, where t_{180} is the 180°-pulse length.

that the effective T_2 measured by the usual 180°-pulse sequences in the same sample is much shorter, of the order of a few milliseconds, since the magnetization is dephased by the ^{13}C-^{13}C couplings.

The effect of the invariance of the total transverse magnetization under the multiple-pulse sequence is dramatic. For the same total 20 ms duration, the magnetization remaining is more than five times higher with the multiple-pulse sequence of Fig. 1b, using 12 cycles with $\tau = 0.8$ ms, than for a single $\tau = 10$ ms cycle of the sequence in Fig. 1a. Note that this increased signal is obtained even though far more pulses are applied in the multiple-pulse sequence.

3.1 Size of Region Probed by Transverse-Magnetization Spin Diffusion

Figure 3a shows a standard 2-D exchange spectrum of the ^{13}COO groups in PVAc at $T = 276$ K with a mixing time of 100 ms. No significant off-diagonal intensity is observed. This shows that on the 100 ms time scale, the "proton-driven" ^{13}C spin diffusion is too inefficient to produce significant transfer of ^{13}C magnetization between ^{13}COO groups of different orientation and frequency.

That the ^{13}C-^{13}C dipolar couplings are intrinsically strong enough to produce such transfer and spin diffusion is proven by the 2-D spectrum in Fig. 3b. It was acquired with 20 ms of transverse-magnetization spin diffusion; otherwise the conditions were the same as for the spectrum in Fig. 3a. Strong off-diagonal intensity and a narrow diagonal ridge are observed, without significant distortions by the multiple-pulse sequence during the mixing time. The projection onto the ω_2-axis is shown at the top of Fig. 3b.

A cross section through the 2-D spectrum, Fig. 3c, with its integral plotted above, shows that the diagonal makes up only 38% of the total intensity. This means that the magnetization has reached two other ^{13}COO groups on average. Since only two out of five carbonyl groups are ^{13}C-labeled, the magnetization probes a region containing five neighboring repeat units. Six [-CH_2-CH{-O-CO-

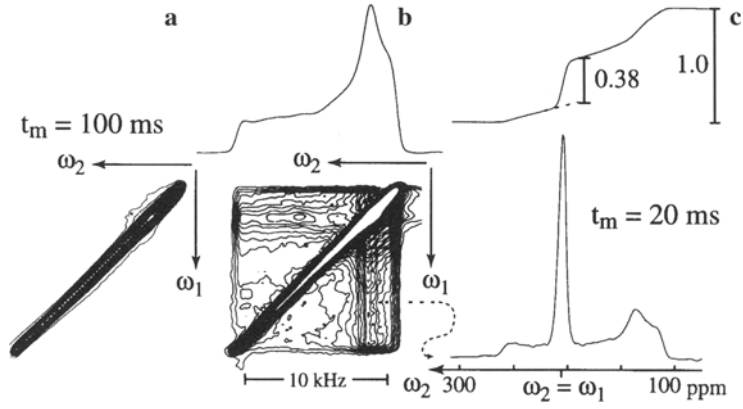

Fig. 3. **a** 2-D spectrum with "proton-driven" spin diffusion during t_m = 100 ms. Contour levels from 1.7% to 100%. No off-diagonal intensity is observed. **b** 2-D exchange spectrum of ^{13}COO-PVAc with transverse-magnetization spin diffusion for t_m = 20 ms (12 cycles of 1.67 ms), obtained with the pulse sequence shown in Fig. 1b and c. The spectrum shows strong exchange intensity. **c** 1-D cross section through the 2-D spectrum in **b**, with integral plotted at the top. The diagonal peak makes up only 38% of the total area.

CH_3}-] units have a molar mass of 516 Da. At a density of 1.2 g/cm^3 = 720 Da/nm^3, they occupy a volume of (0.9 nm)^3, corresponding to a sphere of 1.1 nm diameter. In summary, it is found that 20 ms of transverse-magnetization spin diffusion equilibrate the ^{13}C magnetization within a (0.9 nm)^3 volume.

3.2 Stimulated Echoes

More details on the time dependence of the transverse-magnetization spin diffusion can be obtained by measuring stimulated echoes, using the pulse sequence of Fig. 1b and c with a fixed t_1 = 500 μs and observing the echo at $t_2 = t_1$. The stimulated echo arises from the same ^{13}COO groups as the sharp diagonal ridge in the 2-D spectrum, and its height thus reflects the fraction of magnetization that has not undergone spin diffusion. Figure 4 displays the normalized intensity $s(t_m; t_1 = 500\ \mu s)/s(t_m; t_1 = 1\ \mu s)$ of the stimulated echo, obtained with the pulse sequence of Fig. 1b and c, as a function of the transverse-magnetization spin diffusion time t_m. For an ideal stimulated echo, i.e., without exchange during t_m and without T_2 decay during $t_1 + t_2$, we expect $s(t_m = 1\ ms; t_1 = 500\ \mu s)/s(t_m = 1\ ms; t_1 = 1\ \mu s) = 0.5$ [143]. The experimental data at the shortest mixing time approximate this value within a few percent. At longer mixing times, the stimulated echo is reduced due to diffusion of magnetization from the initial segment to others with different orientations and frequencies. Figure 4 shows that the stimulated-echo height decays to 38% of the initial intensity within 20 ms. This agrees very well with the diagonal fraction of 38% found in the 2-D exchange spectrum, see Fig. 3c.

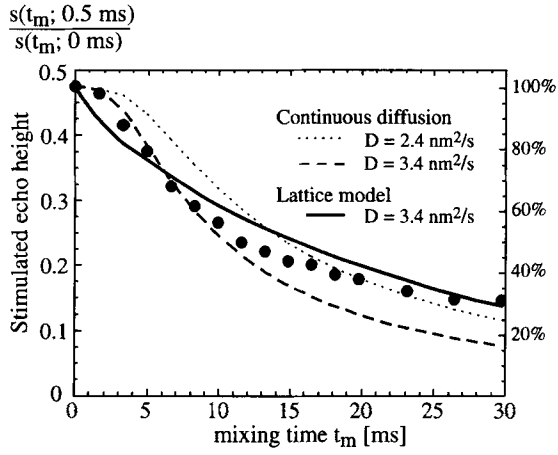

Fig. 4. Relative stimulated-echo intensity $s(t_m;\ t_1 = 500\ \mu s)/s(t_m;\ t_1 = 1\ \mu s)$ as a function of transverse-magnetization spin diffusion time t_m, obtained with the pulse sequence of Fig. 1b and c. This ratio is 0.5 in the absence of exchange and T_2 relaxation during $t_1 + t_2 = 1\ \mu s$, $T = 276$ K. The division by $s(t_m;\ t_1 = 1\ \mu s)$, i.e., by the data shown in Fig. 2, eliminates the effects of T_2 relaxation during the multiple-pulse sequence. Fit curves are for models of continuous Fickian diffusion (dashed curves) with $D = 2.4$ nm^2/ms and $D = 3.4$ nm^2/ms as indicated, and for a random walk on a three-dimensional lattice in continuous time (full line) with $D = 3.4$ nm^2/ms.

3.3 Estimates of the ^{13}C Spin Diffusion Coefficient

Experimentally, we found in the 2-D exchange and the stimulated-echo experiment that after 20 ms of transverse-magnetization spin diffusion, the volume corresponding to the segment in which the magnetization started out contains 38% of the magnetization. This volume is determined through the density and the mass of one segment, divided by 0.4 for dilution, $V_{seg} = m_{seg}/\rho = 86/0.4$ Da/$(1.2 \cdot 600$ Da/nm$^3) = (0.67$ nm$)^3$.

Assuming Fickian diffusion, the distribution of magnetization that started out at the origin is given, at the time t_m, by a normalized Gaussian of width $\sigma = 2Dt_m$ along each of the three orthogonal spatial dimensions. The integral magnetization in the $(0.67$ nm$)^3$ central volume is then

$$M_0(t_m) = \frac{1}{\left(\sqrt{4\pi D t_m}\right)^3} \int_{-0.34\,\mathrm{nm}}^{0.34\,\mathrm{nm}} \int_{-0.34\,\mathrm{nm}}^{0.34\,\mathrm{nm}} \int_{-0.34\,\mathrm{nm}}^{0.34\,\mathrm{nm}} \exp\left(\frac{-(r_1^2 + r_2^2 + r_3^2)}{4Dt_m}\right) \mathrm{d}^3 r \quad . \qquad (15)$$

The diffusion coefficient D can be calculated from $M_0(20\ \mathrm{ms}) = 0.38$. As a first approximation, the integral in Eq. (15) is set equal to the integration volume and one obtains $D \approx (0.67\ \mathrm{nm})^2 (0.38)^{-2/3}/(4\pi \cdot 20\ \mathrm{ms}) = 3.4\ \mathrm{nm}^2/\mathrm{s}$. After a few iterations, $D = 2.4$ nm^2/s is obtained. A similar result is found if dilution is taken into account differently, by considering that the $(0.49$ nm$)^3$ volume of the central segment contains 1/6 of the magnetization.

In Fig. 4, the magnetization $M_0(t_m)$ in the $(0.67\ nm)^3$ "start volume", Eq. (15), is plotted as a function of t_m, for $D = 2.4\ nm^2/s$ and $D = 3.4\ nm^2/s$. The two curves more or less bracket the stimulated-echo data points, but the quality of the fits is not very good. This may be because a continuous Fickian diffusion model is not appropriate at relatively short times t_m when the redistribution of magnetization occurs only between a small number of ^{13}C's.

The discrete nature of the short-time spin exchange process can be taken into account by describing it as discrete random walk in continuous time on a 3-D lattice. The time dependence of the magnetization on each lattice point for the one-dimensional discrete random walk starting at the origin is well known [14, 15]. Since the 3-D random walk can be represented as the product of independent random walks along the three orthogonal spatial dimensions, the magnetization at the origin in the 3-D model can be calculated as

$$M_0^{3D}(t_m) = [M_0^{1D}(t_m)]^3 .$$

It is only a function of the jump (spin exchange) rate Ω, and not of the step size a in the random walk. The diffusion coefficient $D = \Omega a^2$ in this model therefore depends strongly on the step size a. (Note that the continuous-diffusion model also depends on a, since the start volume of a^3 is a crucial parameter.)

The solid line in Fig. 4 shows $M_0^{3D}(t_m)$ for $\Omega = 7.5$ Hz, which compares reasonably well with the typical (i.e., half the maximum) dipolar coupling of 13 Hz expected for an internuclear distance of $a = 0.67$ nm and yields $D = 3.4\ nm^2/s$. It provides a reasonable overall fit to the data; the deviation at short times is expected, since the short-time spin transfer behavior is parabolic in time according to Eq. (2), while the random walk, with a fixed transfer rate, is initially linear in time.

3.4 Comparison between ^1H and ^{13}C Spin Diffusion Coefficients

It is interesting to put the ^{13}C spin diffusion into perspective with the more widely studied case of proton spin diffusion [16]. The typical nearest internuclear ^{13}C-^{13}C distance in the 40% ^{13}COO-labeled PVAc sample is $a = 0.67$ nm, corresponding to a typical ^{13}C-^{13}C dipolar coupling of 12.5 Hz in the weak-coupling limit, to be compared with $\Omega = 7.5$ Hz as found above. The corresponding $a = 0.2$ nm for ^1H in polystyrene yields a typical dipolar coupling of 7.5 kHz (in the sense of Eq. (1); this corresponds to 11 kHz in the very-strong-coupling limit that applies for ^1H wideline spectra). This is slightly smaller than $\Omega = D/a^2 = 13$ kHz found from the experimentally determined $D(^1H) = 0.8\ nm^2/ms$ in polystyrene [16]. Thus, we find in both cases that the transfer rate Ω and the typical dipolar coupling for the given internuclear lattice spacing are of similar magnitude. Nevertheless, the ratios of $\Omega/(\omega_{SL}/2)$ for ^1H and ^{13}C are different by a factor of 2.9.

The spin diffusion coefficient scales with the gyromagnetic ratio γ and the typical smallest internuclear distance a as $D = \Omega a^2 \sim (\gamma^2/a^3)a^2 = \gamma^2/a$. The smaller magnetic moment of ^{13}C leads to a factor of $1/4^2 = 1/16$ reduction of

the ^{13}C transfer rate compared to that for ^{1}H. Combined with the ratio of the a-spacings, $D(^{13}C)/D(^{1}H) = (0.2/0.67)(1/16) = 1/54$. In other words, ^{13}C spin diffusion is expected to be ~ 50 times slower than ^{1}H spin diffusion. With the diffusion coefficient for large domains, $D(^{1}H) = 0.8$ nm^2/ms [16], we calculate $D(^{13}C) = 15$ nm^2/s, which is ~ 4.4 times larger than the experimental value of 3.4 nm^2/s found above; this factor in the diffusion coefficient would correspond to a difference in domain sizes by a factor of $4.4^{1/2} = 2.1$.

The discrepancy in the ratio of the ^{1}H and ^{13}C spin diffusion coefficients arises from the difference in the ratios of the transfer rates and dipolar couplings. This in turn may be due to differences in the spatial distribution of ^{13}C and ^{1}H nuclei. In most polymers, the protonated backbone represents an uninterrupted band of strongly coupled protons which permits efficient spin diffusion.

3.5 Comparison with Spin-Lock Sequences

The ^{13}C spin-diffusion pulse sequence discussed here competes with existing techniques that use radio-frequency-driven ^{13}C spin diffusion. As shown above, the scaling factor of the relevant term in the dipolar coupling for transverse-magnetization spin diffusion is twice as large as under a spin lock. Thus, within half the spin-lock mixing time, similar diffusion will have occurred for the transverse magnetization. Practically speaking, due to its small duty cycle and robust behavior, the pulse sequence of Fig. 1b and c competes favorably with sequences for radio-frequency spin diffusion [3, 4], where sample heating or even hardware damage are a risk for mixing times exceeding 20 ms.

At first sight, it might be expected that transverse relaxation limits the maximum mixing time and thus the maximum spatial range that can be probed with transverse-magnetization spin diffusion, compared to what can be achieved in radio-frequency-driven spin diffusion. However, this assumption is not confirmed by the experimental data. The T_2 relaxation time of ~ 40 ms during the transverse-magnetization spin diffusion found here is very similar to the T_{1r} relaxation time of 40 ms reported for an unprotonated sp^2-hybridized sidegroup carbon in polystyrene [1–4]. Typical mixing times used in the spin-lock experiments are of the order of a few milliseconds [1–4]. Thus, for many purposes, the transverse-magnetization spin diffusion sequence demonstrated here competes favorably with radio-frequency-driven spin diffusion.

4 Conclusions

A robust and efficient multiple-pulse sequence for facilitating dipolar spin diffusion between ^{13}C sites with large chemical-shift anisotropies but weak ^{13}C-^{13}C and ^{13}C-^{1}H dipolar couplings has been demonstrated. The sequence provides for spin diffusion between isochromats of transverse magnetization. It is designed to leave the transverse magnetization invariant in both the weak- and the very-

strong-coupling limit; the decay constant of ~40 ms measured for ^{13}COO groups confirms the success of this scheme. By fortuitous properties of the truncated dipolar Hamiltonian, the scaling factor of the relevant dot-product or "flip-flop" terms in the average dipolar Hamiltonian is unity. Within 20 ms, the magnetization of 40% ^{13}COO-labeled poly(vinyl acetate) equilibrates over a volume of (0.9 nm)^3, or five repeat units. The duty cycle of the pulses applied to ^{13}C is low, <5%, since the sequence contains long windows between pulses, ranging between the inverse ^{13}C-^{13}C dipolar couplings as the upper and the inverse chemical-shift differences as lower limit. The sequence will be useful for ^{13}C spin diffusion in reduced 4-D experiments for determining the sizes of dynamic heterogeneities near the glass transition temperature.

Acknowledgement

This material is based upon work supported by the National Science Foundation under Grant no. DMR-9703916.

References

1. Henrichs P.M., Linder M.: J. Magn. Reson. **58**, 458 (1984)
2. Edzes H.T., Bernards J.P.C.: J. Am. Chem. Soc. **106**, 1515 (1984)
3. Robyr P., Meier B.H., Ernst R.R.: Chem. Phys. Lett. **162**, 417 (1989)
4. Robyr P., Tomaselli M., Straka J., Grob-Pisano C., Suter U.W., Meier B.H., Ernst R.R.: Mol. Phys. **84**, 995 (1995)
5. Tracht U., Wilhelm M., Heuer A., Feng H., Schmidt-Rohr K., Spiess H.W.: Phys. Rev. Lett. **81**, 2727 (1998)
6. Heuer A., Wilhelm M., Zimmermann H., Spiess H.W.: Phys. Rev. Lett. **75**, 2851 (1995)
7. Madi Z.L., Brutscher B., Schulte-Herbruggen T., Bruschweiler R., Ernst R.R.: Chem. Phys. Lett. **268**, 300 (1997)
8. Schulte-Herbruggen T., Madi Z.L., Sorensen O.W., Ernst R.R.: Mol. Phys. **72**, 847 (1991)
9. Waugh J.S., Huber L.M., Haeberlen U.: Phys. Rev. Lett. **20**, 180 (1968)
10. Haeberlen U., Waugh J.S.: Phys. Rev. **175**, 453 (1968)
11. Haeberlen U.: High Resolution NMR of Solids: Selective Averaging. Advances in Magnetic Resonance Supplement 1. New York: Academic Press 1976.
12. Pastawski H.M., Usaj G., Levstein P.R.: Chem. Phys. Lett. **261**, 329 (1996)
13. Schmidt-Rohr K., Spiess H.W.: Multidimensional Solid-State NMR and Polymers. London: Academic Press 1994.
14. Van Kampen N.G.: Stochastic Processes in Physics and Chemistry. Amsterdam: North-Holland 1981.
15. Kentgens A.P.M., de Boer E., Veeman W.S.: J. Chem. Phys. **87**, 6859 (1987)
16. Clauss J., Schmidt-Rohr K., Spiess H.W.: Acta Polymer. **44**, 1 (1993)

Authors' address: Klaus Schmidt-Rohr, Department of Polymer Science and Engineering, University of Massachusetts, Amherst, MA 01003, USA